

RSC Advances



This is an *Accepted Manuscript*, which has been through the Royal Society of Chemistry peer review process and has been accepted for publication.

Accepted Manuscripts are published online shortly after acceptance, before technical editing, formatting and proof reading. Using this free service, authors can make their results available to the community, in citable form, before we publish the edited article. This *Accepted Manuscript* will be replaced by the edited, formatted and paginated article as soon as this is available.

You can find more information about *Accepted Manuscripts* in the [Information for Authors](#).

Please note that technical editing may introduce minor changes to the text and/or graphics, which may alter content. The journal's standard [Terms & Conditions](#) and the [Ethical guidelines](#) still apply. In no event shall the Royal Society of Chemistry be held responsible for any errors or omissions in this *Accepted Manuscript* or any consequences arising from the use of any information it contains.

41 always been the focus [7], among which silicon-containing compounds is considered
42 as a promising choice due to its high flame-retardant efficiency [8,9].

43 As one of the silicon-containing compounds, methyl phenyl silicone resin (Si603)
44 with high thermal stability and carbon residue was selected to modify epoxies.
45 However, it is important to note that, the introduction of polysiloxane flame retardant
46 into the resin not only demonstrated poor compatibility with polymer matrix but also
47 lowered glass transition temperature (T_g) [10]. Therefore, how to overcome these
48 drawbacks without a decrease of the integrated properties of polysiloxane is worth
49 investigating.

50 Recently, Studies on the hyperbranched polymer used as compatibilizer have
51 received a growing prominence. Because of the hybrid inorganic-organic nature
52 [11,12], the hyperbranched polymer possessing epoxy group, which can serve to
53 increase the compatibility with polymers, can improve the thermal stability and the
54 flame retardancy of the EP composites. In addition, the existence of highly reactive
55 groups provides the possibility for chemical modifications [13]. A typical example is
56 the fully end-capped hyperbranched polysiloxane with large branching degree and
57 amine-groups (AmeHBPSi), which was used to modify BMI resin to improve flame
58 retardancy, toughness, strength and thermal stability [14]. Juhua Ye [15] synthesized a
59 novel phosphorus-containing hyperbranched polysiloxane which was then used to
60 improve flame retardancy of cyanate ester resins.

61 The subject of this work is to improve the compatibility of methyl phenyl silicone
62 resin (Si603)/epoxy resin with hyperbranched polymer. Integrated performances
63 (including compatibilization, thermal degradation behavior, and the flame retardancy)
64 of HPSi/methyl phenyl silicone resin/epoxy resin systems were intensively
65 investigated.

66

67 2. Experimental

68

69 2.1. Materials

70

71 Diglycidyl ether of bisphenol A (DGEBA, EP, epoxy value = 0.44 mol/100 g) was
72 purchased from Wuxi Bluestar Chemical Co. Ltd. China. Methyl phenyl silicone resin
73 (Si603) was supplied by WACKER. Germany. γ -(2,3-Epoxypropoxy)
74 propyltrimethoxysilane (KH560) and dimethoxydimethylsilane (DEMS) were bought
75 from Jinan Yijia Chemical Co.Ltd.China. Distilled water,
76 4,4-diaminodi-phenylmethane (DDM), ammonia, and anhydrous ethanol were
77 obtained from Chengdu Kelong Chemical Reagent Factory. All materials were used
78 without further purification.

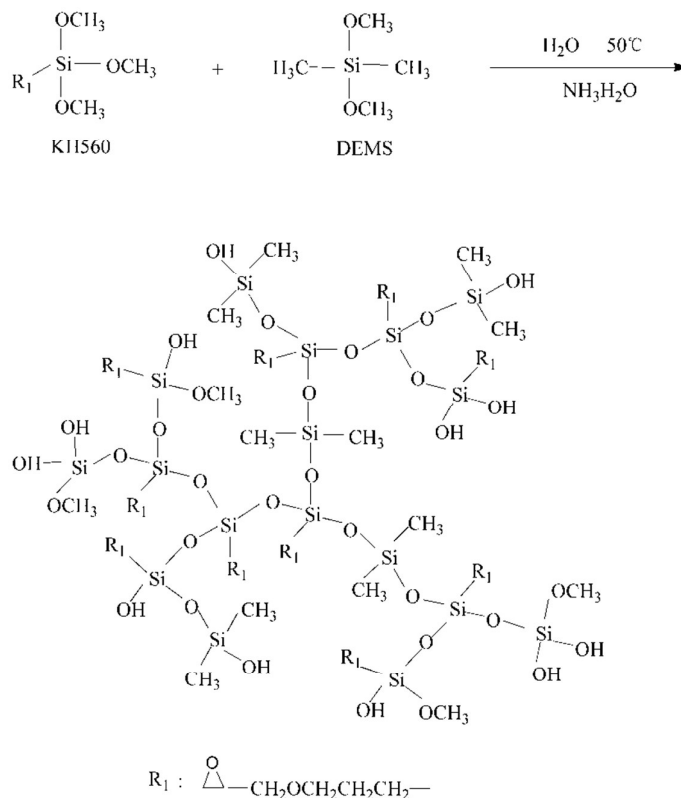
79

80 2.2. Synthesis of polysiloxane (HPSi)

81

82 23.6g KH560, 18g DEMS and 150mL anhydrous ethanol were added to a 250 mL
83 three-necked round bottom flask equipped with a stirrer, a thermometer, and a
84 condenser. Then 0.4g ammonia, 7.56g distilled water were both added into the flask.

85 The temperature was raised to 50 °C and kept for 4.5 h. After that, 0.25g
 86 1-chlorotrimethylsilane was added as capping agent. Finally, the product was dried to
 87 eliminate methanol, ethanol, and water in a vacuum oven. Finally, a transparent and
 88 viscous liquid, hyperbranched polysiloxane (coded as HPSi), was obtained. The
 89 reaction mechanism of this system is shown in Scheme 1.



90
 91 **Scheme 1** The synthesis of organic silicon resin (HPSi) by hydrolytic condensation.

92 93 2.3. Preparation of cured HPSi/EP/Si603/DDM blends

94
 95 HPSi and epoxy with a ratio at 0.1:1(mass) was blended with vigorous stirring at
 96 130 °C for 20 min to obtain a prepolymer. Then an appropriate amount of Si603 (10
 97 wt%, 20 wt%, 30 wt%) was put into the above prepolymer. Third, stoichiometric
 98 DDM was casted into the blends above to dissolve at 100 °C. Subsequently, the
 99 blends were cast into a preheated aluminium mold for curing and postcuring
 100 following the protocol of 80 °C/2 h+ 150 °C/3.5 h+165 °C/1.5 h. Then epoxy resin
 101 specimens were obtained and subsequently machined to the desirable size for further
 102 testing.

103 104 2.4. Measurements

105 106 Fourier transform infrared spectra

107
 108 Fourier transform infrared spectra(FTIR) were recorded between 400 and 4000

109 cm^{-1} on a Nicolet Magna-IR 560 spectrometer (Nicolet Instrument Co, USA) with
110 KBr chip technique.

111

112 Nuclear magnetic resonance

113

114 ^1H -NMR (400 Hz) spectra were recorded on a FT-80A NMR with CDCl_3 as the
115 solvent and internal standard.

116

117 Differential scanning calorimetry

118

119 DSC measurements were conducted on a Netzsch Q-200 ranging from room
120 temperature to 350°C with a heating rate of $10^\circ\text{C min}^{-1}$ under nitrogen atmosphere.

121

122 Scanning electron microscopy

123

124 The morphologies of the fractured surfaces of samples and the surface morphology
125 of the char obtained after the LOI tests were observed by Inspect-F SEM.

126

127 Thermogravimetric analysis

128

129 TG analyses were conducted on Netzsch TG209 at a linear heating rate of 10 K
130 min^{-1} under pure nitrogen and air within the temperature range from 30 to 800°C .

131

132 Limiting oxygen index

133

134 LOI data of all samples were obtained at room temperature on an oxygen index
135 instrument (XYC-75) produced by Chende Jinjian Analysis Instrument Factory,
136 according to GB/T2406-93 standard. The dimensions of all samples were $130 \times 6.5 \times$
137 3 mm^3 .

138

139 Vertical burning tests

140

141 Vertical burning tests were performed according to UL-94 standard with samples of
142 dimensions $125 \times 12.5 \times 3.2 \text{ mm}$. In this test, samples were classed as V-0, V-1, V-2,
143 or unclassified according to their behaviour (dripping of burning material and burning
144 time).

145

146 Mechanical properties

147

148 Tensile and flexural tests were carried out on a Shimadzu AGS-J universal testing
149 machine, according to ASTM D638-08 and ASTM D-790. The rate of crosshead
150 motion was $20 \pm 2 \text{ mm min}^{-1}$. The tensile and flexural tests of environmental chamber
151 were performed at 25°C . Samples' dimensions were $80 \times 10 \times 4 \text{ mm}^3$. For each
152 mechanical test, the result was averaged by testing at least 10 samples. The result was

153 calculated based on the data after subtracting the data outside the margin of standard
154 deviation.

155

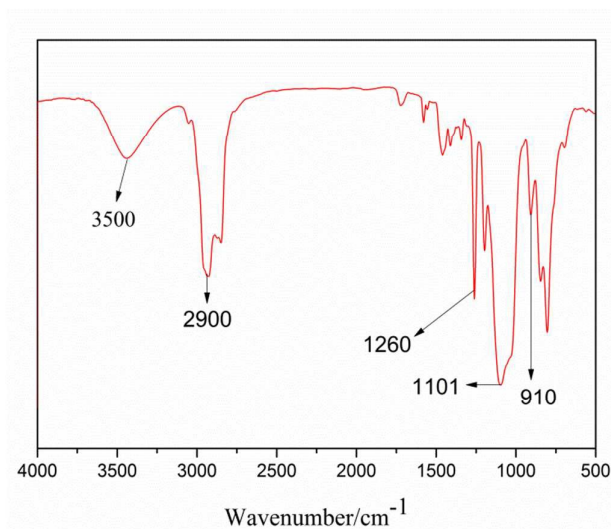
156 3. Results and discussion

157

158 3.1. Synthesis and characterization of HPSi

159

160 In order to confirm the molecular structure of HPSi, FTIR, $^1\text{H-NMR}$ analyses were
161 carried out. Figure 1 is the FTIR spectrum of HPSi. The FTIR spectrum of HPSi
162 shows that the strong and wide peak at 1101 cm^{-1} was attributed to bending vibration
163 of Si-O-Si groups, indicating that alkoxy groups were successfully changed into Si-
164 O-Si through the hydrolysis and condensation; however the broad peak centered at
165 3500 cm^{-1} representing Si-OH groups can also be observed, demonstrating that Si-OH
166 groups in the raw material do not completely disappear during the condensation [16].
167 The emergence of the chemical shift at 2.79 ppm assigning to -OH groups in the
168 $^1\text{H-NMR}$ of HPSi (Figure 2) also supports this statement. Moreover, a stretching
169 vibration of the oxirane ring group at 910 cm^{-1} demonstrates that the polymerization
170 between KH560 and DEMS occurred. We can also see that a vibration peak (2840 cm^{-1})
171 assigns to methoxy, and the peaks in the range of $750\text{ to }870\text{ cm}^{-1}$ indicate the
172 existence of Si-CH₃. To further prove the structure of HPSi, Figure 2 shows the
173 $^1\text{H-NMR}$ spectrum of HPSi (ppm): 2.6 (a), 2.79 (b), 3.18 (c), 3.67 (d), 3.32 (e), 3.48
174 (f), 1.62 (g), 3.52(k), 0.67 (i), 7.12-7.66 (j) [17]. It suggests that the HPSi is
175 successfully synthesized.



176

177

Figure 1 The FTIR of HPSi.

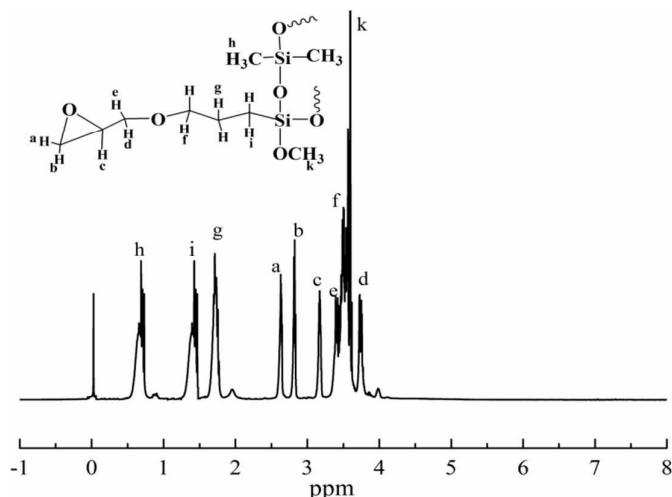


Figure 2 The ^1H -NMR of HPSi.

178

179

180

181 3.2. Compatibility of cured HPSi/EP/Si603/DDM blends

182

183 Compatibility of EP/Si603/DDM improved by HPSi can be characterized by
184 measuring the glass transition temperature (T_g). Generally speaking, the homogeneous
185 morphology of the mixed epoxy systems exhibit only one T_g , while incompatible
186 mixtures exhibit two or more T_g . Differential scanning calorimetry (DSC) can
187 accurately detect the T_g of the blends [18]. Figure 3 gives DSC curves of various
188 cured EP/Si603/DDM, EP/HPSi/DDM, EP/HPSi/Si603/DDM mixtures.
189 EP/Si603/DDM exhibits two separated T_g at 74 and 154 °C, which are close to the T_g
190 of Si603 and pure epoxy resin, respectively. Except EP/Si603, the rest of the curing
191 systems have a single T_g between 119 and 127 °C, which indicates that HPSi greatly
192 improved the compatibility of this system. This phenomenon mainly interpreted by
193 the fact that HPSi contains a large amount of epoxy groups and Si-O-Si bonds, which
194 have the similar structure with EP and Si603 resin, respectively. It can also be
195 observed that with the increase of Si603, T_g of the whole system increases until
196 reaches the maximum value of 127 °C, following which is an obviously decreases.
197 Owing to a relatively large space volume, Si603 resin usually has higher average free
198 volume that plays a negative role in increasing the concentration of the chain segment
199 of modified resins. At the same time, in the case of the EP/Si603/HPSi/DDM system,
200 there are strong interactions between Si603 and HPSi, which can conspicuously
201 increase the packing density of the polymer. The positive factor is dominant when the
202 content of Si603 is between 10 and 20 wt%, while when the content of Si603
203 increases from 20 to 30 wt% the negative factor will offset this positive effect. From
204 the data analysis of characterize scanning calorimetry (DSC), the addition of HPSi
205 successfully improves the compatibility of EP/Si603/DDM, which provides the
206 important prerequisite for Si603 as a flame retardancy of EP.

207

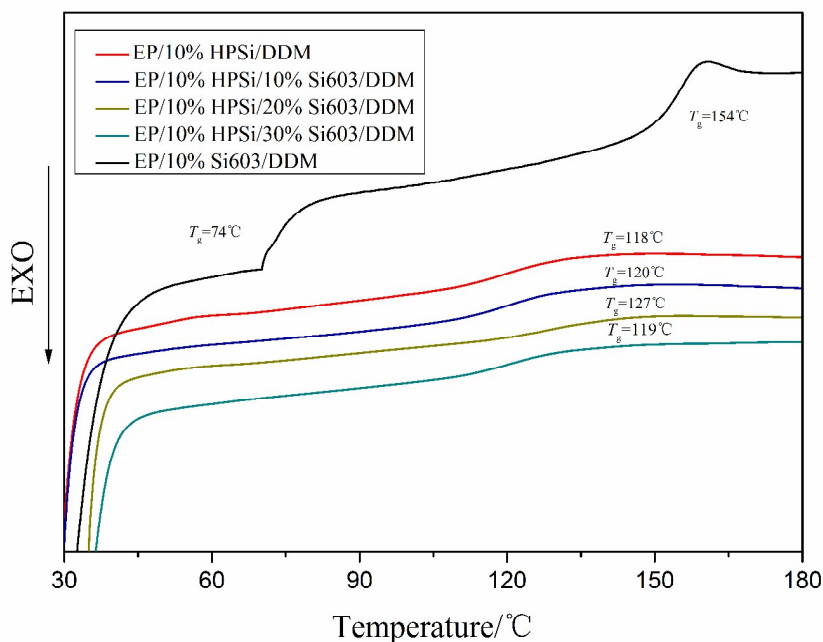
208

209

To further explore the influence of HPSi in the cured system, SEM morphologies of the fractured surfaces of samples are shown in Figure 4. The sample of EP/Si603/DDM resin is laminated with the translucent yellow bottom and the white

210 opaque upper. Figure 4a is the SEM photograph of EP/30%Si603/DDM cured sample.
 211 Holes and balls are almost invisible because Si603 have migrated to the surface of the
 212 matrix in the process of blending and curing. In addition, reuniting in the process of
 213 blending was also responsible for the serious phase separation. Such phenomena
 214 demonstrated the poor compatibility of EP/Si603, Si603 can't be well dispersed in the
 215 EP matrix in the absence of compatibilizer. Morphology of the EP/10%HPSi/DDM
 216 cured sample shows the compact, smooth, and tight surface in Figure 4b which
 217 demonstrates the outstanding compatibility of EP/HPSi.

218 Cured EP/10%HPSi/30%Si603/DDM is transparent and uniform yellow. It can
 219 be observed in Figure 4c that the fractured surface is flat. What's more, small balls
 220 and circular holes appear on the fractured surface. These balls are evenly distributed
 221 in the matrix, which could be attributed to that the Si603 is ideally dispersed in EP
 222 matrix in the presence of HPSi. After placed in anhydrous ethanol for 20 hours , a
 223 large number of circular holes appear on the fractured surface of
 224 EP/10%HPSi/30%Si603/DDM (Figure 4d), which is caused by the dissolution of part
 225 of the balls occupied by Si603 resin.
 226



227
 228 **Figure 3** The DSC curves of the blending systems.
 229
 230
 231
 232
 233

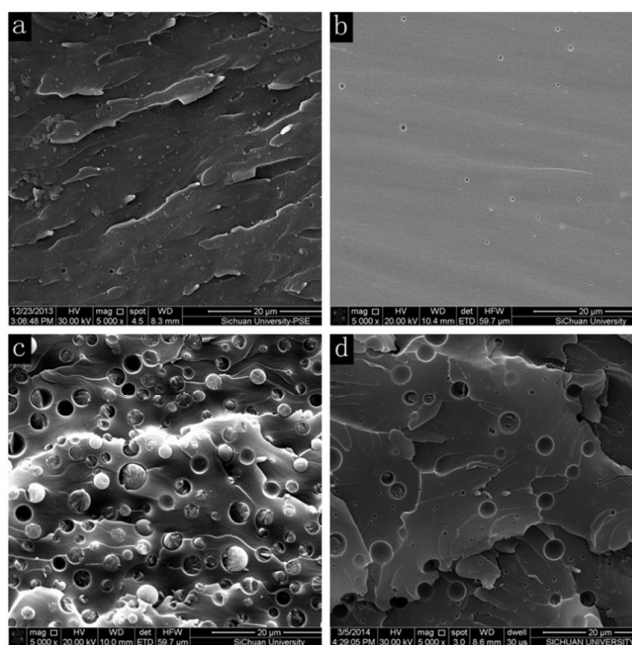


Figure 4 SEM of the section of the blending systems.

234

235

236

237 3.3. Flammability

238

239

240

241

242

243

244

245

246

247

248

249

250

251

252

253

254

Table 1 The values of LOI and UL-94 for finally cured systems

Sample	LOI (%)	UL-94	255
EP/DDM	21.5	NR	
EP/10%HPSi/DDM	23	NR	
EP/10% HPSi /10%Si603/DDM	26	V-2	
EP/10% HPSi /20%Si603/DDM	28.5	V-2	
EP/10% HPSi /30%Si603/DDM	31	V-1	

256

257 3.4. Thermal analysis

258

259 TG and DTG traces of cured EP/HPSi/Si603/DDM systems provided additional
260 information in regard to their thermal stability and thermal degradation behavior [20].
261 The thermal degradation behavior of the various samples in nitrogen atmosphere are
262 shown in Figure 5. The corresponding $T_{5\%}$, the T_{\max} , and char yield (Y_c) at 800 °C are
263 summarized in Table 2. $T_{5\%}$ represents the temperature at which mass loss is 5 % for
264 the system (the initial decomposition temperature), $T_{1\max}$ and $T_{2\max}$ represents the
265 temperature of the first maximum mass loss rate for the system and the second
266 maximum mass loss rate for the system, respectively. Y_c represents the char yields at
267 800 °C

268 It can be observed from Figure 5 that all cured resins except HPSi have one-stage
269 decomposition process, demonstrating that the original and modified EP resins have
270 similar degradation processes.

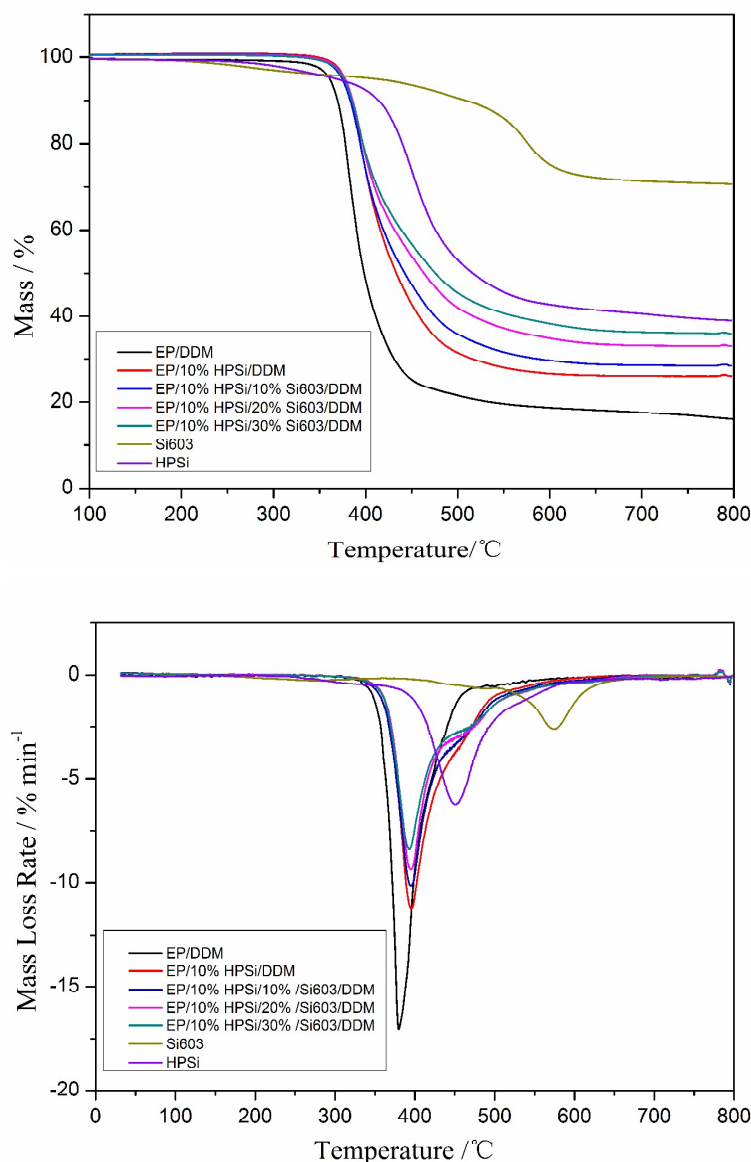
271 Figure 5 shows that the char residue at 800°C is 39 % and $T_{5\%}$ and T_{\max} of cured
272 HPSi is 368°C and 457°C, respectively. The degradation of HPSi in nitrogen
273 atmosphere has gone through two processes: unzipped degradation occurs before 400°C
274 and following silicone chain scission rearrangement [21]. When terminal hydroxyl
275 groups exist, a poorer heat resistance of the silicone resin is presented. As can be seen
276 from the FTIR spectrum of HPSi (Figure 1), HPSi contains a small amount of
277 silicone hydroxy, which can initiate unzipped degradation through backbiting reaction,
278 which mainly produces low molecular weight annulations and thus thermal weight
279 loss happens. A small amount of unzipped degradation occurred during the
280 degradation processes probably because HPSi contains a large number of branches,
281 which greatly reduce the occurrence of unzipped degradation. At 457°C, cured HPSi
282 shows a T_{\max} , which is mainly caused by the cleavage and rearrangement reaction of
283 Si-O-Si bonds.

284 TG shows that the addition of HPSi (10 wt%) enhances the thermal stability of
285 EP/DDM system: $T_{5\%}$ and $T_{1\max}$ of EP/HPSi/DDM are higher than that of EP/DDM.
286 This phenomenon originates from the decomposition of HPSi at inferior temperature
287 (368°C) that leads to the formation of the silicone-containing group, which will
288 participate in the cross-linked carbonization. Moreover, the Si-O group of HPSi is
289 able to absorb more thermal energy and its vibration could dissipate the thermal
290 decomposition energy [22]. However, with the increase of Si603 resin, $T_{5\%}$ and $T_{1\max}$
291 of EP/HPSi/Si603/DDM systems are almost the same. While char residue at 800°C
292 remarkably increases from 16.01 % to 35.88 % with Si603 content increases from 0%
293 to 30 %. As being discussed above, silicone resins have the ability to convert the usual
294 organic decomposition to partially inorganic decomposition by forming the
295 carbon-silicon residue acting as thermal insulation [11,12,23,24] to prevent gas
296 evolution, and achieve ultimate improvement on flame retardation of this
297 silicone-containing epoxy system.

298

299

300



301

302

303

304

Figure 5 The TG and DTG curves of the cured systems under N₂ atmosphere.

305

306

307

308

309

310

311

312

313

314

315

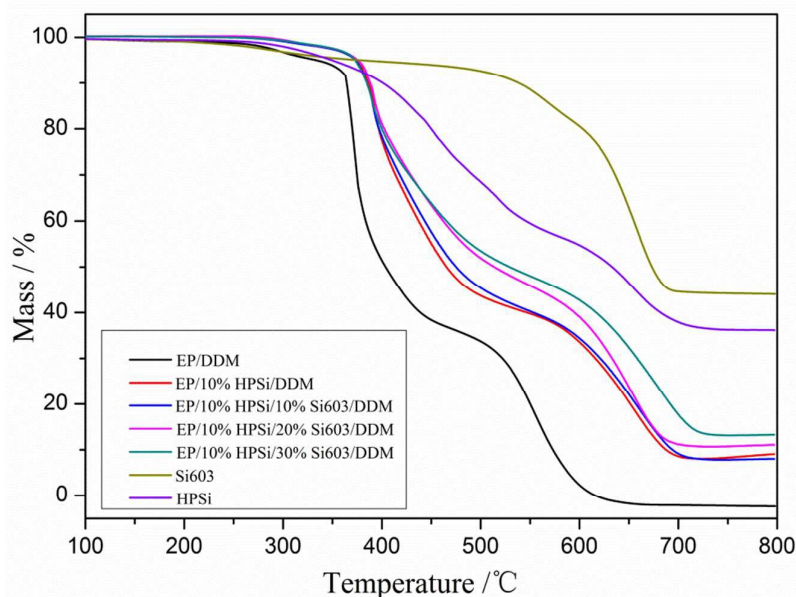
Figure 6 depicts the TG and DTG curves of cured EP/DDM, HPSi and EP/HPSi/Si603/DDM resins in air atmosphere and the corresponding $T_{5\%}$, the T_{\max} , and char yield (Y_c) at 800 °C are summarized in Table 3.

As can be seen that HPSi experiences three stages of degradation processes which occur at the temperature range of 300-510 °C, 510-600 °C and 600-750 °C in air atmosphere, the largest thermal degradation peaks appear at 452 °C, 540 °C and 653 °C. When the temperature reaches 350 °C, initial decomposition occurs and the char yield is 36.16% when the temperature reaches 800 °C. Thus, due to the presence of oxygen, the decomposition mechanism of cured HPSi has changed. For HPSi in air atmosphere, thermo-oxidative degradation occurs, which includes thermal degradation of the main chain and the oxidation reaction of the organic groups. As can

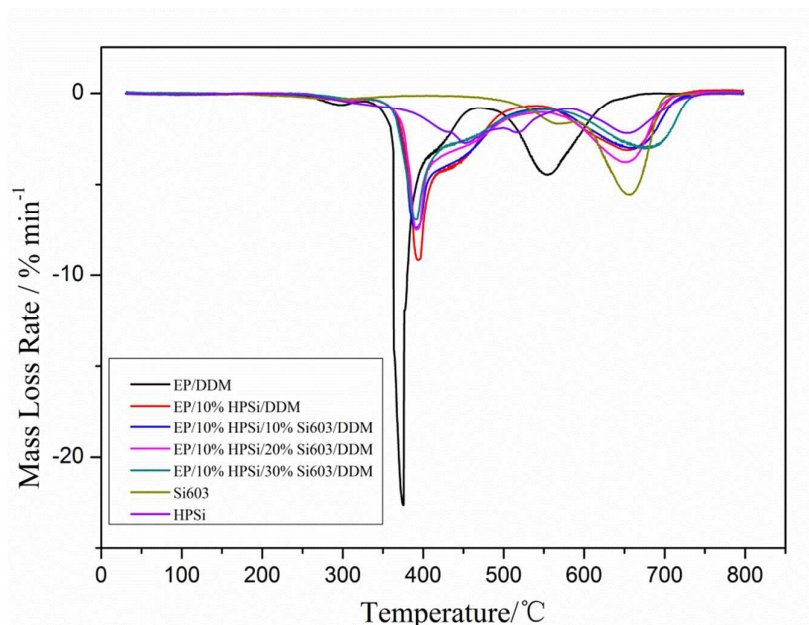
316 be seen from the figure that before the main chain degradation (600 °C), the two
317 peaks appear, which due to the thermo-oxidative degradation of the side groups,
318 generating small molecules such as carbon monoxide, carbon dioxide, water and so
319 on.

320 For EP/DDM resin, bits of decompositions appear before 300 °C, which can be
321 attributed to the decomposition of unstable alkyl groups in the hybrids. The chain
322 scission of the isopropylidene linkage takes place, leading to the release of EP and its
323 derivates at the initial decomposition stage [25]. The thermal degradation of EP resin
324 can be divided into two independent steps: the first thermal decomposition occurs
325 between 362 and 470 °C, the second stage is from 470 to 700 °C with 0 % char
326 residue at 800 °C, which demonstrates that pure EP shows poor charring ability.

327 But the initial thermal decomposition of EP/HPSi/Si603/DDM systems, occurring
328 between 350 and 600 °C, are wider than that of EP/DDM resin, and the second stage
329 are from 600 to 700 °C. What's more, T_{max} of EP/HPSi/Si603/DDM systems become
330 higher, especially the, with the content of Si603 resin increasing. The improvement can
331 be attributed to silicon in the condensed phase which leads to the formation of a
332 surface glassy char acting as a barrier to heat and mass transfer at high temperature.
333 As is shown in Table 3, as the content of Si603 increases, the char residue of the
334 overall system significantly enhances; when the amount of Si603 increases from 0 %
335 to 30 %, the char residue of EP/HPSi/Si603/DDM system combusted in air
336 atmosphere increases from 0 % to 13.21 %, indicating that HPSi enhances the thermal
337 stability and char formation ability of EP. This is reasonable as we can see from the
338 TG curve that Si603 resin possesses high thermal stability. When it is over 400 °C,
339 decomposition occurs in Si603 resin and the solid char yield in nitrogen and air
340 at 800 °C is 70 % and 44 %, respectively. It demonstrates that charring ability and
341 thermal stability of Si603 resin is significantly higher than that of other resins.



342



343

344

Figure 6 The TG and DTG curves of the cured systems under air atmosphere.

346

347

348

Table 2 The TG and DTG data of different systems under N₂ atmosphere.

Sample	$T_{5\%}$	R_{1peak}	T_{1max}	Y_c at 800°C	
	/ °C	/ (%°C ⁻¹)	/ °C	Cal.	Exp.
EP/DDM	350.8	-17.07	379	---	16.01
Si603	410	-5.22	574	---	70
HPSi	368	-6.22	460	---	39
EP/10%HPSi/DDM	377.5	-11.24	396	18.1	25.99
EP/10%HPSi/10%Si603/DDM	375	-10.16	395	21.34	28.5
EP/10% HPSi /20%Si603/DDM	376	-9.39	395	26.08	32.94
EP/10% HPSi /30%Si603/DDM	376.2	-8.39	393	29.22	35.88

349

350

351

352

353

354

355

356

357

358

Table 3 The TG and DTG data of different systems under air atmosphere.

Sample	$T_{5\%}$	R_{1peak}	T_{1max}	R_{2peak}	T_{2max}	Y_c at 800°C	
	/ °C	/ % °C ⁻¹	/ °C	/ % °C ⁻¹	/ °C	Cal.	Exp.
EP/DDM	334	-22.59	375	-4.47	555	—	0
Si603	380	-5.43	566	-4.06	656	—	44
HPSi	350	-2.76	452	-2.20	653	—	36.16
EP/10%HPSi/DDM	373.5	-9.18	394	-3.13	654	3.29	9.08
EP/10%HPSi/10%Si603/DDM	374	-7.43	390	-3.06	661	6.68	9.85
EP/10% HPSi /20%Si603/DDM	375	-7.52	391	-3.79	654	9.55	11.1
EP/10%HPSi/30%Si603/DDM	373	-6.95	392	-3.06	674	12	13.21

359

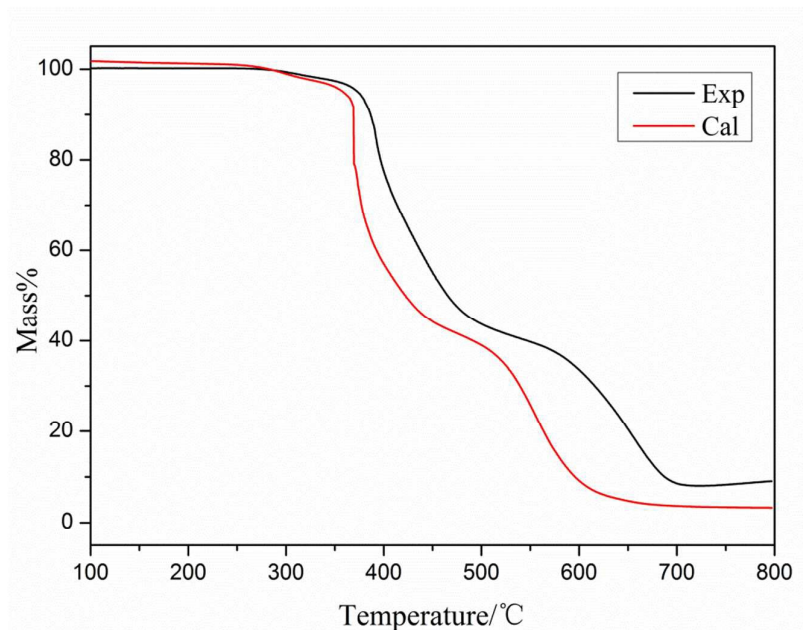
360 Figure 7 and Figure 8 show the experimental and theoretical TG curves of
 361 EP/10%HPSi/30%Si603/DDM system in N₂ and air, respectively. The theoretical
 362 curve was calculated based upon the mass percentage of the ingredient in the EP
 363 system. The formula is as follows:

$$364 M_{cal} = wt_{HPSi}\% * M_{HPSi\ exp} + wt_{EP}\% * M_{EP\ exp} + wt_{Si603}\% * M_{Si603\ exp}$$

365 M_{cal} is the theoretical amount of carbon residue, M_{exp} refers to the actual amount of
 366 carbon residue, wt% refers to the corresponding proportion of ingredients.

367 As can be seen in N₂, when the temperature is below 350 °C, the experimental and
 368 theoretical curves are similar. However, the experimental mass of residual char
 369 exceeds the theoretical one after 400 °C. The experimental and theoretical TG curves
 370 of EP/HPSi/Si603/DDM system in air are different after 350 °C: the experimental
 371 mass of residual char surpasses the theoretical one in the whole temperature range and
 372 both decomposition stages occurs at higher temperatures. It could be deduced that the
 373 addition of organic silicon obviously improves the mass of carbon residue and organic
 374 silicon generates more stable substance at high temperatures, which effectively
 375 improves the char-formation ability and thermal stability of the matrix.

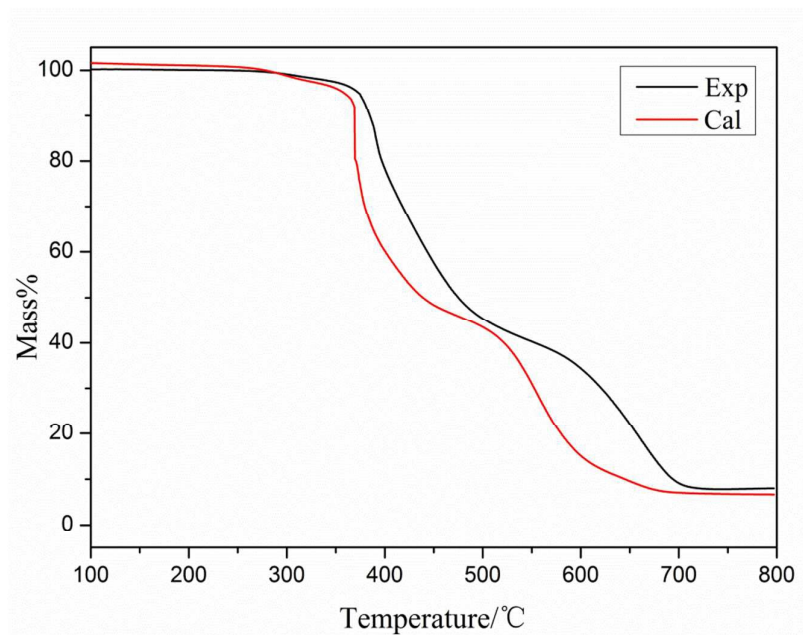
376 Higher char yield of Si603 resin indicates that the carbonization mechanism
 377 indeed plays an important role in flame retardation. It is well known that the general
 378 flame retarding mechanism of organic silicone resin-based materials is thought to be
 379 the formation of protective barrier during combustion. The improved flame retardancy
 380 can be explained by a flame retarding mechanism: providing a barrier for heat and
 381 mass transfer in the condensed phase at the same time preventing melted EP from
 382 burning [26].



383

384 **Figure 7** Experimental and theoretical TG curves of EP/10% HPSi/30%Si603 under
385 N₂ atmosphere.

386



387

388 **Figure 8** Experimental and theoretical TG curves of EP/10% HPSi/30%Si603 under
389 air atmosphere.

390

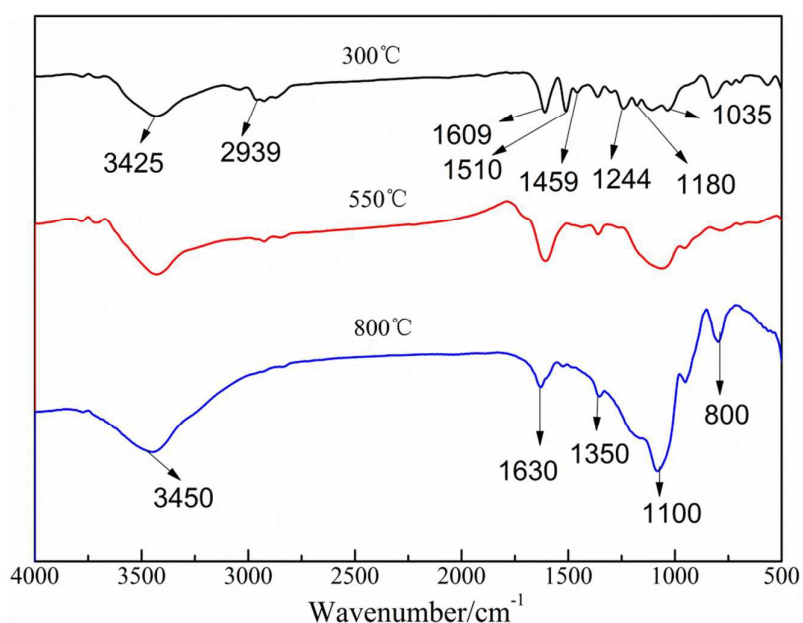
391 3.5. Structural analysis of the combustion residue by FTIR

392

393 In order to understand the chemical alteration in the condensed phase of
394 EP/10%HPSi/30%Si603/DDM system, the combustion residue after

395 thermogravimetry under air atmosphere were investigated by FTIR. The FTIR spectra
 396 at different degradation temperatures (300, 550 and 800 °C) are shown in Figure 9.

397 At 300 °C, the absorptions of –OH (3450 cm^{-1}), stretching vibration of –CH₃ and –
 398 CH₂– (2939 cm^{-1}), C–C stretching vibration of aromatic ring (1609, 1510, 1459 cm^{-1}),
 399 C–H vibration of –C₆H₄–O–CH₂– (1244, 1035 cm^{-1}) and C–O stretching vibration
 400 (1180 cm^{-1}) are the characteristic absorptions of pure epoxy resin [27]. At 550 °C, it is
 401 found that the absorption peaks at 2939, 1609, 1459, 1244 and 1035 cm^{-1} disappear
 402 and the decrease in the relative intensities of the aromatic components related bonds
 403 (1510 cm^{-1}) and ether bonds (1180 and 1035 cm^{-1}) were detected, indicating that the
 404 main decomposition happened in this stage. which is consistent with the TG results.
 405 According to the shown information, the absorption of aliphatic components and the
 406 C–C stretching vibration of aromatic ring at 1510 cm^{-1} totally disappear at 800 °C.
 407 However, bending vibration peak belonging to Si–O–Si groups centered at 1100 cm^{-1}
 408 become stronger and wider and characteristic peaks belonging to polyaromatic
 409 centered at 800 cm^{-1} and 1630 cm^{-1} become broader, indicating the formation of
 410 polyaromatic carbons.
 411



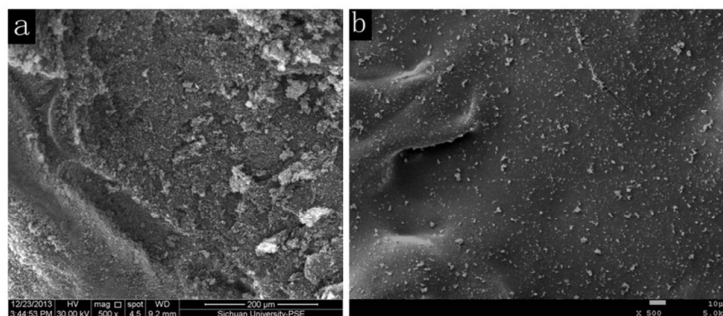
412 **Figure 9** The FTIR of char layer of EP/10% HPSi/30%Si603/DDM.
 413
 414

415 3.6. Morphology of the residue char

416
 417 In order to explore how the structure of char determines the flame retardancy of EP,
 418 we investigated the residues of char after LOI testing by SEM. Figure 10 presents
 419 SEM micrographs of char residue of EP/10%HPSi/30%Si603/DDM and EP/DDM.
 420 According to Figure 10a, for cured EP, there are many big holes due to insufficient
 421 char formation or less condensed char during the burning process. This poor char
 422 quality could not effectively protect the underlying EP from degradation during
 423 combustion; therefore, EP can't pass UL 94-V0. However, the char surface of EP with

424 both HPSi and Si603, illustrated in Figure 10b, is compact, smooth, and tight. This
425 structure of the char for EP composites could prevent heat transfer between the flame
426 Si603 and the substrate and thus protect the underlying materials from further burning
427 and pyrolysis, which endows the material much higher LOI values. In addition, this
428 char structure could offer a good shield to prevent melted EP from burning, which
429 was proved in vertical flammability tests (Table 1).

430



431

432 **Figure 10** SEM of the char layer of EP/DDM and EP/10%HPSi/30%Si603/DDM
433 system.

434

435

436 3.7. Mechanical properties

437

438 Tensile strength is a measurement of the force required to pull sample to the point
439 where it breaks, and reflects the fracture resistance of materials. Flexural strength is
440 usually used for evaluating the mechanical properties of a material because the
441 flexural loading is very complicated and may contain multi-type loadings such as
442 tensile, shearing and/or compressing loadings [28]. Therefore, to evaluate the
443 integrated mechanical properties of a material, flexural strength is usually selected as
444 a typical parameter to evaluate the integrated mechanical properties. The flexural
445 modulus reflects the inherent energy of a material, and the ability to resist strain.
446 Moreover, it is also a property reflecting the stiffness of a material [29]. Therefore,
447 flexural modulus is usually selected as typical parameters to evaluate the stiffness of
448 the materials [29, 30].

449 The tensile strength, flexural strength and flexural modulus of
450 EP/HPSi/Si603/DDM composites are compared and the results are presented in Table
451 4. Overall, a continuous reduction in flexural strength, tensile strength and flexural
452 modulus showed up as the addition of Si603 increases. However, there is only an
453 almost negligible decline in the tensile strength, flexural strength and flexural
454 modulus of EP/10%HPi/10%Si603/DDM compared with that of the EP/DDM, which
455 is attributed to the better compatibility of EP/Si603/DDM improved by HPSi and the
456 improved homogeneity of the system to some extent offset the negative effect the
457 Si603 brings to the mechanical property. As the addition of Si603 increased, the
458 reduction in tensile strength, flexural strength and flexural modulus are obviously
459 observed. Owing to a large amount of unoccupied structure, a hyperbranched polymer
usually has higher average volume of free cavities that play a negative role in

460 decreasing the concentration of the chain segment of modified resins and the large
 461 number of rigid pendant groups (benzene rings) from Si603 decreased the flexibility
 462 of the compound provided by the siloxane linkages, hence the EP/HPSi/Si603/DDM
 463 with a large content of Si603 (>20 wt%) possesses decreased toughness. These results
 464 are in line with those in literature, in detail, a suitable content of
 465 phosphorus-containing flame retardant will contribute a satisfactory flame retardancy
 466 to a resin, but meanwhile, which usually brings a negative effect on the flexural
 467 strength of the resin system [31,32].

468

469 **Table 4** Mechanical properties of EP/10%HPSi/Si603/DDM system with different
 470 Si603 contents

Specimen	Mechanical properties		
	Tensile strength /MPa	flexural strength /MPa	flexural modulus /MPa
EP/DDM	45.87	97.77	3579.6
EP/10%HPi/10%Si603/DDM	45.03	97.55	3553.5
EP/10% HPSi/20%Si603/DDM	40.76	89.57	3326.7
EP/10% HPSi/30%Si603/DDM	29.56	68.92	3182.6

471

472 **4. Conclusions**

473

474 A novel hyperbranched polysiloxane (HPSi) with epoxy groups was successfully
 475 synthesized as compatibilizer by controlling hydrolysis and condensation between
 476 c-(2,3-epoxypropoxy) propyltrimethoxysilane (KH560) and dimethoxydimethylsilane
 477 (DEMS). Experiments suggested that HPSi significantly improved compatibility of
 478 EP/Si603/DDM systems.

479 What's more, a series of EP/10%HPSi/Si603/DDM hybrids containing 0 wt%, 10
 480 wt%, 20 wt% and 30 wt% content of Si603 were prepared. The flame retardancy of
 481 the products was examined by an LOI measurement and UL-94 vertical test. LOI
 482 value of EP/10%HPSi/30%Si603/DDM was 31, which was about 1.4 times of the
 483 corresponding value of neat EP, and a V-1 grade for the UL-94 can be achieved. TG
 484 showed that the addition of HPSi (10 wt%) enhanced the thermal stability of
 485 EP/DDM system.

486 The high silicon content and rich aromatic group structures of Si603 contributed an
 487 excellent flame retardancy to epoxy resins. Specifically, the char residues of the
 488 EP/10%HPSi/30%Si603/DDM system could reach 35.88 % in N₂ and 13.21 % in air
 489 at 800 °C. Structural analysis of the combustion residue by FTIR indicated the
 490 formation of polyaromatic carbons which slowed heat and mass transfer between the
 491 gas and condensed phases. Based on this, the speculated degradation process of
 492 silicon resin was obtained. These properties would make this epoxy attractive for
 493 practical applications such as flame-retardant laminates.

494

495

496 **Acknowledgments**

497

498 We would like to thank the generous supports by the following: Sichuan Applied
499 Basic Research Program; the Experiment Center of Polymer Science and Engineering
500 Academy, Sichuan University;

501

502

503

504

505

506 [1] Jones RR, London: Chapman & Hall, 1993, **8**, 256-302

507 [2] Morell M, Ramis X, Ferrando F, Yu YF and Serra A, *Polymer*, 2009, **50**, 5374–
508 5383.

509 [3] Wetzell B, Hauptert F and Qiu Zhang M, *Compos. Sci. Technol.*, 2003, **63**, 2055–
510 2067.

511 [4] Rosu D, Cascaval CN, Mustata F and Ciobanu C, *Thermochim. Acta.* 2002, **383**,
512 119–127.

513 [5] Wang WJ, Perng LH, HPSiue GH and Chang FC, *Polymer*, 2000, **41**, 6113.

514 [6] HPSiue GH, Wang WJ and Chang FC, *J. Appl. Polym. Sci.*, 1999, **73**, 1231.

515 [7] Gojny FH, Wichmann MHG, Fiedler B, Kinloch IA, Bauhofer W, Windle AH and
516 Schulte K, *Polymer*, 2006, **47**, 2036–2045.

517 [8] Smith SD, Long TE and McGrath JE, *J. Polym. Sci., Part A:* 1994, **32**, 1747–1753.

518 [9] Kambour RP, Klipfer HJ and Smith SA, *J. Appl. Polym. Sci.*, 1981, **26**, 847.

519 [10] Lin ST and Huang SK, *J. Polym. Res.*, 1994, **1**, 151.

520 [11] Wang X, Hu Y, Song L, Xing WY and Lu HD, *J. Polym. Sci. Polym. Phys.*, 2010,
521 **48**, 693–705.

522 [12] Chiang CL and Ma CCM, *Polym. Degrad. Stab.*, 2004, **83**, 207.

523 [13] Mahapatra S and Singha KN, *J. Mater. Sci., Part A:* 2009, **46**, 296-303.

524 [14] Zhuo D, Gu A, Liang G, Hu J, Yuan L and Chen X, *J. Mater. Chem.*, 2011, **21**,
525 6584-6594.

526 [15] Juhua Ye, Guozheng Liang, Aijuan G* and Zhiyong Zhang, *Polym. Degrad. Stab.*,
527 2013, **98**, 597-608.

528 [16] Zhang GB, Fan XD, Liu YY, Kong J and Wang SJ, *J. Polym.*, 2007, **7**, 644–646.

529 [17] Torry SA, Campbell A, Cunliffe AV and Tod DA, *Int. J. Adhes.*, 2006, **26**, 40–49.

530 [18] Wang WJ, Perng LH, HPSiue GH and Chang FC, *Polymer*, 2000, **41**, 6113–6122.

531 [19] Ying Ling Liu, Yie Chan Chiu and Chuan Shao Wu, *J. Appl. Polym. Sci.*, 2003,
532 **87**, 404 – 411.

533 [20] Tang Z, Li Y and Zhang YJ, *Polym. Degrad. Stab.*, 2012, **97**(4), 638-644.

534 [21] Howard TT, Kenick T C, *J. Polym. Sci. Part B: Polym Phys*, 1969, **7**, 537–549

535 [22] Curry JE and Byrd JD, *J. Appl. Polym. Sci.*, 1965; **9**, 295.

536 [23] Kanai H, Sullivan V and Auerback A, *J. Appl. Polym. Sci.*, 1994, **53**, 527.

537 [24] Kambour RP, Ligon WV and Russell RP, *J. Polym. Sci., Part C:* 1978, **16**, 327.

538 [25] Wu CS, Liu YL and Chiu YS, *Polymer*, 2002, **43**, 4277–4284.

- 539 [26] Kambour RP, J. Appl. Polym. Sci., 1981, **26**, 861.
- 540 [27] Wang X, Hu Y, Song L, Xing WY, Lu HD and Lv P, Polymer, 2010, **51**, 2435–
- 541 2445.
- 542 [28] Xavier S, Misra A, Polym Compos., 1985, **6**, 93-9.
- 543 [29] Karthikeyan C, Sankaran S, Polym. Adv., 2007, **18**, 254-6.
- 544 [30] Shao Q, Lee-Sullivan P, Polym. Test., 2000, **19**, 239-50.
- 545 [31] Chen ZK, Yang G, Yang JP, Fu SY, Ye L, Huang YG, Polymer., 2009, **50**,
- 546 1316-23.
- 547 [32] Li B, He J, Polym. Degrad. Stab., 2004, **83**, 241-6.